Inorganica Chimica Acta 414 (2014) 53–58

Contents lists available at ScienceDirect

Inorganica Chimica Acta

journal homepage: www.elsevier.com/locate/ica

Structures and magnetic studies of two new bimetallic chain complexes constructed by manganese(III)–(Schiff-base) and *mer*-tricyanidoferrate building block

Yingying Wang [a], Hongbo Zhou [a], Xiaoping Shen [a,*], Aihua Yuan [b]

[a] School of Chemistry and Chemical Engineering, Jiangsu University, Zhenjiang 212013, China
[b] School of Material Science and Engineering, Jiangsu University of Science and Technology, Zhenjiang 212003, China

ARTICLE INFO

Article history:
Received 2 November 2013
Received in revised form 13 January 2014
Accepted 22 January 2014
Available online 6 February 2014

Keywords:
Manganese complex
Iron complex
Tricyanidoferrate
Crystal structure
Magnetic property

ABSTRACT

Two new cyano-bridged bimetallic complexes, $\{[Mn^{III}(5\text{-}CH_3)salen][Fe^{III}(qcq)(CN)_3]\}_n \cdot 1.85H_2O$ (**1**) [salen = *N*,*N*′-ethylenebis(salicylideneiminato) dianion; qcq^- = 8-(2-quinoline-2-carboxamido)quinoline anion] and $\{[Mn^{III}(acphen)][Fe^{III}(qcq)(CN)_3]\}_n \cdot 6.46H_2O$ (**2**) (acphen = bis(*o*-hydroxyacetophenone) ethylenediiminate), have been synthesized and characterized both structurally and magnetically. The structures of **1** and **2** are both 1-D zigzag chains connected through π···π stacking and short contact interactions to form extended supramolecular networks. The magnetic measurements revealed the presence of antiferromagnetic $Fe^{III}\cdots Mn^{III}$ interactions in **1** and **2**. Interestingly, weak slow magnetic relaxation was only detected for **1**, indicating the intermolecular antiferromagnetic interactions in **2** are stronger than that in **1** and lead to the disappearance of the 1-D magnetic behavior.

1. Introduction

Low dimensional magnets have still been one of the largest interests for chemists and physicists because of their fantastic property and potential applications in molecular devices, high-density information storage and quantum computer, etc. [1–4]. Nevertheless, the most difficulties encountered are the rather low T_B (Blocking Temperature) and their complicated magneto-structural correlation. To clarified the magnetic mechanism of such low dimensional systems (0-D or 1-D), a great number of related complexes have been thoroughly investigated [5–14]. For the research field, Mn^{III}(Schiff-base) cations are especially remarkable because they have contributed to the first several Single Chain Magnets (SCMs) as reported by Miyasaka and co-workers [15,16]. The results indicated that the slow magnetic relaxations observed were originated from large uniaxial anisotropy of Mn^{III} and significant intrachain exchange interactions without spin compensation between the high-spin magnetic units. To date, many building blocks especially the cyanometalates were used to react with Mn^{III}(Schiff-base) cations, affording a large number of relevant magnetic complexes [17–56]. However, it is still a challenge to fully understand both the structure and magnetism of these complicated systems. For example, the intramolecular Fe^{III}–CN–Mn^{III} exchange coupling could be found as ferro- [25–29] or antiferromagnetic [28–33], where both the intra-/intermolecular contributions and the local anisotropy derived from molecular topology make the systems complicated and no very clear magneto-structural correlation in this type of systems has been established. Consequently, it is still very important and meaningful to synthesize more related low dimensional complexes to provide sufficient experimental references to clarify these problems.

Under this background, we have focused on the magnetic assemblies based on Mn^{III}(Schiff-base) cations and tricyanidoferrate anions such as $[Fe^{III}(qcq)(CN)_3]^-$(qcq^- = 8-(2-quinoline-2-carboxamido) quinoline anion) (Scheme 1). Two new cyano-bridged bimetallic complexes, $\{[Mn^{III}(5\text{-}CH_3)salen][Fe^{III}(qcq)(CN)_3]\}_n \cdot 1.85H_2O$ (**1**) [salen = *N*,*N*′-ethylenebis(salicylideneiminato) dianion; qcq^- = 8-(2-quinoline-2-carboxamido)quinoline anion] and $\{[Mn^{III}(acphen)][Fe^{III}(qcq)(CN)_3]\}_n \cdot 6.46H_2O$ (**2**) (acphen = bis(*o*-hydroxyacetophenone)ethylenediiminate), have been synthesized and characterized both structurally and magnetically. Hererin, we report the syntheses, crystal structures and magnetic properties of the two new 1-D chain complexes.

2. Experimental

2.1. Reagents and materials

All chemicals and solvents used in this study were reagent grade and were used without further purification. $K[Fe^{III}(qcq)(CN)_3]$,

* Corresponding author. Fax: +86 511 88791800.
E-mail address: xiaopingshen@163.com (X. Shen).

http://dx.doi.org/10.1016/j.ica.2014.01.046
0020-1693/

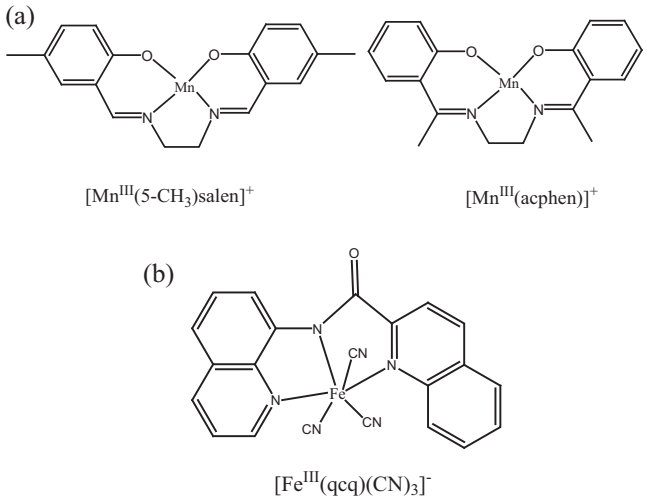

Scheme 1. (a) Mn^{III}(Schiff-base) cations used in this work; (b) The $[Fe^{III}(qcq)(CN)_3]^-$ anion.

$PPh_4[Fe^{III}(qcq)(CN)_3]$, $[Mn^{III}(5\text{-}CH_3)salen(H_2O)]ClO_4$ and $[Mn^{III}(acphen)(H_2O)]ClO_4$ were synthesized according to the methods reported previously [32,57].

Caution! Cyanides are highly toxic and perchlorate salts of metal complexes are potentially explosive. So handing them carefully with small quantities is highly suggested for the safety consideration.

2.2. Synthesis of complex $\{[Mn^{III}(5\text{-}CH_3)salen][Fe^{III}(qcq)(CN)_3]\}_n \cdot 1.85H_2O$ (**1**)

An acetonitrile solution (5 mL) of $[Mn^{III}(5\text{-}CH_3)salen(H_2O)]ClO_4$ (0.01 mmol) was slowly added into an aqueous solution (5 mL) of $K[Fe^{III}(qcq)(CN)_3]$ (0.01 mmol) with constant stirring. After about 10 min, the brown mixture obtained was filtered and the filtrate was kept undisturbed in the dark. Two weeks later, the black block crystals suitable for X-ray diffraction were formed and carefully collected by filtration, washed with 1:1 (v/v) acetonitrile/water, and dried at room temperature. Anal. Calcd for $C_{40}H_{33.7}FeMnN_8O_{4.85}$: C, 58.96; H, 4.17; N, 13.75; Fe, 6.85; Mn, 6.74. Found: C, 58.53; H, 4.24; N, 13.57; Fe, 6.98; Mn, 6.77%. IR: ν_{max}/cm^{-1}: 3444(s), 2130(m), 1620(s), 1540(m), 1504(w), 1465(m), 1446(m), 1390(m), 1342(w), 1290(m), 1211(m), 1151(m), 900(w), 769(m).

2.3. Synthesis of complex $\{[Mn^{III}(acphen)][Fe^{III}(qcq)(CN)_3]\}_n \cdot 6.46H_2O$ (**2**)

An acetonitrile solution (5 mL) of $[Mn^{III}(acphen)(H_2O)]ClO_4$ (0.01 mmol) was slowly added into a methanol/water (v:v = 1:1) solution (5 mL) of $PPh_4[Fe^{III}(qcq)(CN)_3]$ (0.01 mmol) with constant stirring. The mixture was treated using the same procedure as **1**. Two weeks later, the black prism crystals suitable for X-ray diffraction were obtained and carefully collected by filtration, washed with 1:1 (v/v) acetonitrile/water, and dried at room temperature. *Anal.* Calc. for $C_{40}H_{42.92}FeMnN_8O_{9.46}$: C, 53.51; H, 4.82; N, 12.50; Fe, 6.22; Mn, 6.12. Found: C, 53.63; H, 4.84; N, 12.45; Fe, 6.25; Mn, 6.10%. IR: ν_{max}/cm^{-1}: 3444(s), 2131(m), 1619(s), 1540(m), 1503(w), 1462(m), 1445(m), 1390(m), 1340(w), 1292(m), 1211(m), 1150(m), 900(w), 765(m).

2.4. Physical Measurements

Elemental analyses for C, H and N were carried out at a Perkin-Elmer 240C analyzer. Mn, Fe analyses were performed on a Jarrell-Ash 1100 + 2000 inductively coupled plasma quantometer (ICP). IR spectra were recorded on a Nicolet FT-170SX spectrometer with KBr pellets in the 4000–400 cm^{-1} region. All magnetic measurements on microcrystalline samples (13.54 and 8.34 mg for **1** and **2**, respectively) were conducted on a Quantum Design MPMP-XL7 superconducting quantum interference device (SQUID) magnetometer. Corrections of measured susceptibilities were carried out considering both the sample holder as the background and the diamagnetism of the constituent atoms [-407×10^{-6} cm^3 mol^{-1} for **1** and -454×10^{-6} cm^3 mol^{-1} for **2**, respectively (per $Fe^{III}Mn^{III}$)] according to Pascal's tables [58].

2.5. X-ray structure determination

Diffraction data were collected on a Bruker *SMART APEX CCD* area detector diffractometer using graphite-monochromated Mo Kα radiation (λ = 0.71073 Å) with the φ and ω scan mode. Structures were solved using direct method and refined by a full-matrix least-squares techniques based on F^2 using SHELXL-97 [59]. All non-hydrogen atoms were refined with anisotropic thermal parameters. The H atoms of chelated ligands were calculated at idealized positions and included in the refinement in a riding mode with U_{iso} for H assigned as 1.2 (or 1.5) times U_{eq} of the attached atoms. The water oxygen atoms O4, O5, O6 in complex **1** and O4, O5, O7, O8 in **2** (H-atoms are not found) are not present with unit occupancy, and it is allowed an anisotropic free variable refinement with partial occupancy. The crystallographic data and experimental details for structural analyses are summarized in Table 1.

3. Results and discussion

3.1. Description of the structures

The important structural parameters such as key bond distances and angles are listed in Table 2. The crystal structures of complexes **1** and **2** are shown in Fig. 1. The intermolecular interactions and packing structures are depicted in Figs. S1–S2 in the Supplementary imformation.

Table 1
Details of the crystallographic data collection, structural determination and refinement for **1**–**2**.

	1	**2**
Formula	$C_{40}H_{33.7}FeMnN_8O_{4.85}$	$C_{40}H_{42.92}FeMnN_8O_{9.46}$
F_W	814.83	897.88
Crystal system	monoclinic	monoclinic
Space group	$P2(1)/c$	$P2(1)/c$
a (Å)	17.394(2)	16.678(3)
b (Å)	17.023(3)	13.303(3)
c (Å)	13.053(4)	22.804(8)
α (°)	90.00	90.00
β (°)	91.42(3)	124.79(2)
γ (°)	90.00	90.00
V (Å^3)	3863.8(14)	4155.1(19)
Z	4	4
D_{calc} (g cm^{-3})	1.394	1.414
$F(000)$	1676	1810.7
θ (°)	1.17–25.00	3.06–25.00
Index ranges	$-20 \leqslant h \leqslant 20$	$-19 \leqslant h \leqslant 19$
	$-17 \leqslant k \leqslant 20$	$-15 \leqslant k \leqslant 12$
	$-15 \leqslant l \leqslant 15$	$-27 \leqslant l \leqslant 17$
Total/unique data	26437/6762	19538/7261
Observed data		
$[I > 2(I)]$	4333	6172
R_{int}	0.0682	0.0661
Data/restraints		
/parameters	4333/0/509	6172/0/550
Goodness-of-fit (GOF) on F^2	1.012	1.008
$R_1[I > 2\sigma(I)]$	0.0794	0.0920
wR_2 (all data)	0.1697	0.1880

Table 2
Selected bond lengths (Å) and angles (°) for **1**–**2**.

1		**2**	
Fe1–C1	1.946(6)	Fe1–C1	1.951(7)
Fe1–C2	1.935(6)	Fe1–C2	1.926(6)
Fe1–C3	1.959(7)	Fe1–C3	1.965(7)
Fe1–N4	2.009(6)	Fe1–N4	1.965(5)
Fe1–N5	1.900(5)	Fe1–N5	1.884(5)
Fe1–N6	2.025(6)	Fe1–N6	2.008(5)
Mn1–O2	1.881(4)	Mn1–O2	1.871(4)
Mn1–O3	1.865(4)	Mn1–O3	1.858(4)
Mn1–N1$^{\#1}$	2.334(5)	Mn1–N1	2.277(5)
Mn1–N2	2.269(5)	Mn1–N2$^{\#2}$	2.270(5)
Mn1–N7	1.983(6)	Mn1–N7	1.996(5)
Mn1–N8	1.998(5)	Mn1–N8	2.007(5)
Fe1–C1–N1	175.2(6)	Fe1–C1–N1	178.7(6)
Fe1–C2–N2	173.9(6)	Fe1–C2–N2	171.8(6)
Fe1–C3–N3	179.4(7)	Fe1–C3–N3	175.3(6)
Mn1–N1$^{\#1}$–C1	151.2(5)	Mn1–N1–C1	159.1(5)
Mn1–N2–C2	160.2(5)	Mn1–N2$^{\#2}$–C2	161.5(5)

Symmetry transformations used to generate equivalent atoms: #1: x, $0.5 - y$, $0.5 + z$; #2: $1 - x$, $-0.5 + y$, $1.5 - z$.

Complexes **1** and **2** both crystallize in the monoclinic $P2(1)/c$ space groups and have comparable structures but they are not isomorphism. As shown in Fig. 1, each of $[Fe^{III}(qcq)(CN)_3]^-$ anions adopts two *cis*-cyanido groups to coordinate axially to two Mn^{III}(Schiff-base) cations, while each of Mn^{III}(Schiff-base) cations links to two $[Fe^{III}(qcq)(CN)_3]^-$ anions in *trans*-mode, affording the zigzag chain arrangements. The chain styles are also comparable to some other relevant complexes built by Mn^{III}(Schiff-base) cations and tricyanidoferrate building blocks, where the differences between them are the different function groups used [30,32–37].

For the $[Fe^{III}(qcq)(CN)_3]^-$ moieties, the central Fe^{III} ion is located in a distorted octahedral environment defined by the tridentate N-donor ligand qcq^- and three cyano groups. The Fe–C(cyanide) bond lengths [**1**: 1.935(6)–1.959(7) Å; **2**: 1.926(6)–1.965(7) Å] are close to each other, but the Fe–N(qcq) bond distances deviate from each other. The relatively shorter Fe–N(qcq) bond distances for Fe1–N5 (amide) [**1**: 1.900(5) Å; **2**: 1.884(5) Å] than that for Fe1–N3/N4 (aromatic rings) [**1**: 2.009(6)–2.025(6); **2**: 1.965(5)–2.008(5) Å] can be often observed and should be due to the strong σ-donor effect of the deprotonated amide [32]. Like most tricyanidoferrate

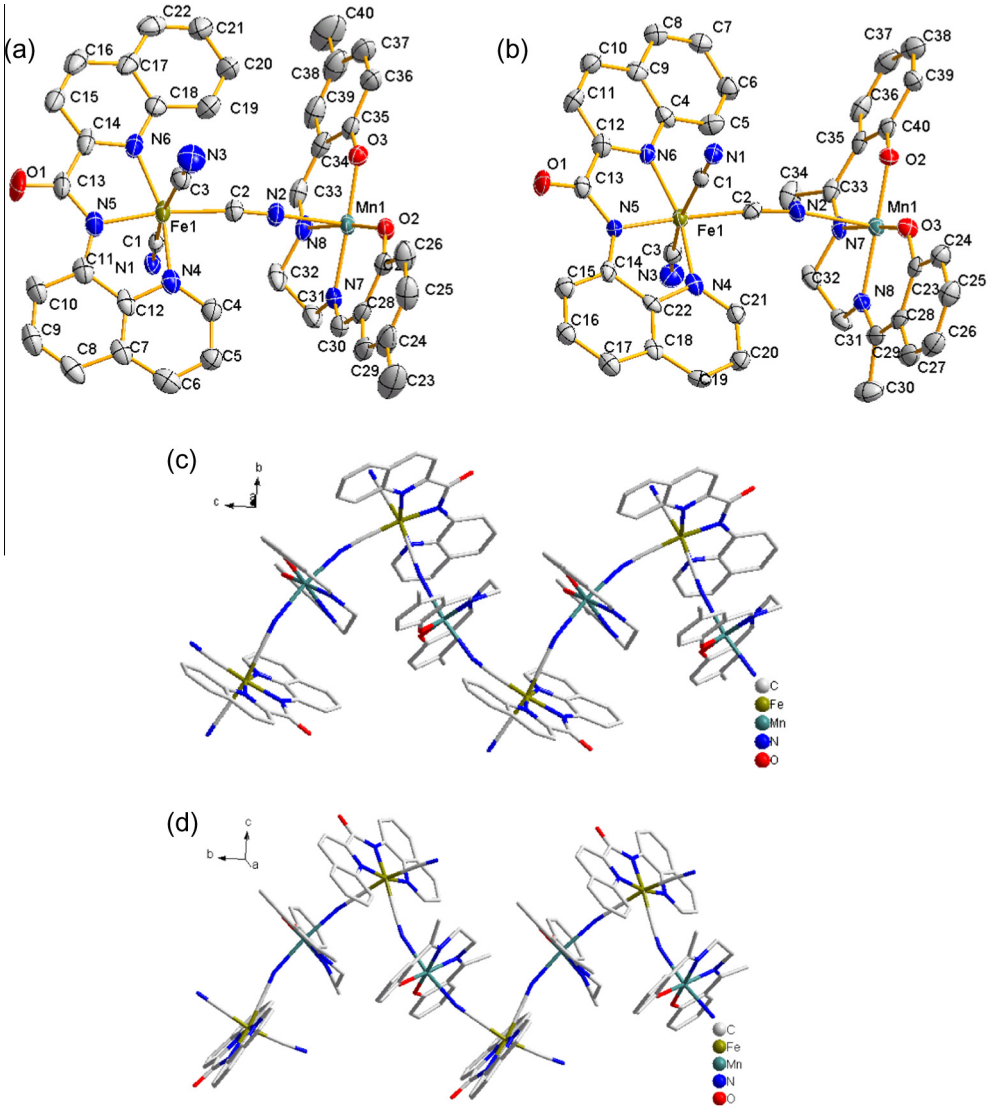

Fig. 1. ORTEP (30%) diagrams of asymmetric units with selected atom-labeling schemes for **1** (a) and **2** (b), and the 1-D chain structures for **1** (c) and **2** (d) (hydrogen atoms and crystallized solvent molecules are omitted for clarity).

based bimetallic complexes [30,32–37], the Fe–C≡N bond angles remain almost linear [**1**: 173.9(6)–179.4(7)°; **2**: 171.8(6)–178.7(6)°]. For **1**, the terminal CN group of Fe1–C3≡N3 show the largest angle of 179.4°(7), while that for **2** are only 175.3(6)°, hydrogen bond interaction of C3–N3···O4 in **2** should be responsible for such distortion. As for the Mn^{III}(Schiff-base) moiety, the Mn^{III} ion locates in centre of highly elongated octahedron (Jahn–Teller effect) with the equatorial plane occupied by four N_2O_2 donor atoms [**1**: Mn1–O2 = 1.881(4) Å, Mn1–O3 = 1.865(4) Å, Mn1–N7 = 1.983(6) Å, Mn1–N8 = 2.001(5) Å; **2**: Mn1–O2 = 1.871(4) Å, Mn1–O3 = 1.858(4) Å, Mn1–N7 = 1.996(5) Å, Mn1–N8 = 2.007(5) Å] from the Schiff base ligand and apical positions coordinated by two N atoms [**1**: Mn1–$N1^{\#1}$ = 2.334(5) Å, Mn1–N2 = 2.269(5) Å;**2**: Mn1–N1 = 2.277(5) Å, Mn1–$N2^{\#2}$ = 2.270(5) Å (#1: x, $0.5-y$, $0.5+z$; #2: $1-x$, $-0.5+y$, $1.5-z$)] from the cyanide groups of two neighboring [Fe^{III}(qcq)$(CN)_3$]$^-$ units. The Mn–N≡C(cyanide) angles for **1** and **2** are equal to 151.2(5)–160.2(5)° and 159.1(5)–161.5(5)°, respectively, which show obvious deviation from linear and comparable to the similar systems [30,32–37]. The intrachain Fe···Mn distances through the CN bridges are 5.23–5.25 Å for **1** and 5.29 Å for **2**, respectively.

For the packing structures of **1** and **2**, interchain π–π stacking is observed (Figs. S1–S2). The chains interact with each other *via* the face to face stacking of adjacent aromatic rings from [Fe^{III}(qcq)$(CN)_3$]$^-$ (centroid to centroid distance: 3.6–3.7 Å for **1**; 3.5–3.6 Å for **2**), resulting in the formation of 3-D supermolecualr networks. Besides, hydrogen bond interactions are also presented in **1** and **2**, but it is not possible to analyze them in detail because the water hydrogen atoms were not found by the X-ray determination. The shortest interchain metal–metal separations are 8.5–9.2 Å for **1** and 8.5–8.6 Å for **2**, respectively, indicating that the pairs of chains are more closely packed in the crystal structure of **2** than in **1**.

3.2. Magnetic properties

Polycrystalline samples of **1** and **2** were used for the measurement of the dc magnetic susceptibility data, as shown in Fig. 2 (a, b). At room temperature, the $\chi_M T$ values are 3.2 and 3.4 cm^3 $K\,mol^{-1}$ for **1** and **2**, respectively, in agreement with the spin-only value of 3.375 cm^3 $K\,mol^{-1}$ expected for magnetically diluted spin system of one low spin Fe^{III} (s_{Fe} = 1/2) and one high spin Mn^{III} (S_{Mn} = 2) assuming $g_{Fe} = g_{Mn} = 2.0$. The room temperature $\chi_M T$ values for **1** and **2** indicate the contributions of residual orbital degeneracy of Fe^{III} should be weak and insignificant. Upon cooling, the $\chi_M T$ product for **1** gradually decreases until reach a quasi-plateau of 2.8 cm^3 $K\,mol^{-1}$ at around 10 K, and then an additional sudden decrease of the $\chi_M T$ value is observed at lower temperatures. Different from **1**, the $\chi_M T$ value for **2** continuously decrease upon cooling until reach a minimum of 0.5 cm^3 $K\,mol^{-1}$ at 1.8 K. The $\chi_M T$ thermal behavior of **1** and **2** is typical of dominant intrachain antiferromagnetic couplings between the Mn^{III} and Fe^{III} spin carriers [28–33]. In the low temperature region, **2** does not show ferrimagnetic behavior expected for ferrimagnetic chain, which could be ascribed to the presence of intermolecular antiferromagnetic interactions and/or zero field split effect.

To evaluate quantitatively the magnitude of the intrachain Fe···Mn interactions (J) within the chain, the magnetic data of **1** and **2** have been modeled using an isotropic Heisenberg Hamiltonian (Eq (1), with $S_{Mn,i} = S_{Mn,i+1} = 2$ and $s_{Fe,i} = 1/2$) based on the approach introduced by Seiden [60,61] for alternating chains of quantum spins s = 1/2 and classical spins S = 2.

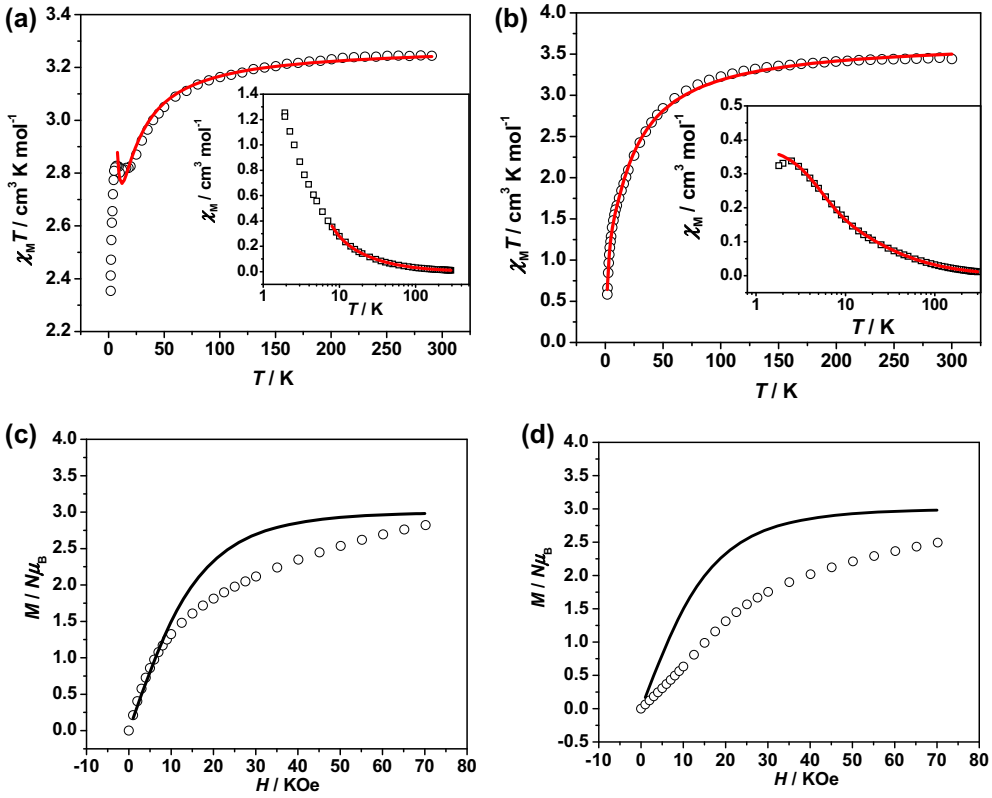

Fig. 2. Temperature dependence of $\chi_M T$ and χ_M (inset) for **1** (a) and **2** (b) measured at 2 kOe (The red solid lines represent the best fits to the models described in the text); Field dependence of the magnetization for **1** (c) and **2** (d) at 1.8 K (The black solid line represent the theoretical Brillouin curves calculated from antiferromagnetic $Fe^{III}Mn^{III}$ unit). (For interpretation of the references to colour in this figure legend, the reader is referred to the web version of this article.)

$$H = -J\sum_{-\infty}^{+\infty}(S_{Mn,i}s_{Fe,i} + S_{Fe,i}S_{Mn,i+1}) \quad (1)$$

For **1**, the data in the temperature range of 10–300 K have been used for fitting, giving the set of parameters, $J = -3.7$ cm^{-1}, $g_{Mn} = g_{Fe} = 1.99$. It can be seen that the 1-D infinite regular chain model could reproduce the data above 20 K well, clearly suggesting the 1-D magnetic behavior above 20 K. No acceptable fitting result can be obtained for the low temperature magnetic data (1.8–20 K) even if the interchain exchange interactions (zJ') were introduced in the model in the mean field approximation (Eq. (2)) [58].

$$\chi = \frac{\chi_{MnFe}}{1 - [2zj'/(Ng^2\mu_B^2)]\chi_{MnFe}} \quad (2)$$

Different from **1**, the susceptibility data of **2** could be well fitted down to 1.8 K by introducing the interchain exchange interaction of zJ' (Eq. (2)) in the Seiden model, affording $J = -4.75$ cm^{-1}, $g_{Mn} = g_{Fe} = 2.08$, $zJ' = -1.5$ cm^{-1}. The zJ' value seems to be overestimated because the magnetic anisotropy brought by the Mn^{III} ions can also contribute to the downturn of the $\chi_M T$ values [16]. Besides, the J values should also be taken with caution because of the overestimated zJ' value. From the obtained result, the complex of **2** does show structurally 1-D chain arrangement but are better described as 3-D networks from a magnetic point of view at least below 20 K.

To further study the low temperature magnetic property, field-dependent magnetization measurement (0–70 kOe at 1.8 K) was then performed [Fig. 2 (c, d)]. For **1** and **2**, the magnetization increases with the increasing external field and reaches 2.82 $N\mu_B$ and 2.50 at 70 kOe, respectively. The values at 70 kOe are consistent with the theoretical saturated value ($3N\mu_B$, calculated from $M_S = g(S_{Mn}–S_{Fe})$ with $g = 2$) expected for an antiferromagnetic coupling of the Mn^{III} ($S_{Mn} = 2$) and Fe^{III} ($s_{Fe} = 1/2$) spins along the chain. For comparison, the theoretical Brillouin curves calculated from antiferromagnetic Fe^{III}Mn^{III} unit were also plotted (Fig. 2c), which also reveal that dominant antiferromagnetic Mn$^{III}\cdots$Fe^{III} couplings are presented along the chain.

The investigation of the dynamic properties [Alternating current (AC) magnetic measurements] reveal that complex **1** (Fig. 3) shows detectable frequency dependent χ''_M signals at low temperature, indicating the presence of slow magnetic relaxations at the very low temperature. However, only frequency independent χ'_M and χ_M'' signals were detected for **2** (Fig. S3), revealing the disappearance of such slow magnetic relaxations that were observed in **1**.

From the above structural and magnetic analysis, it is found that **1** and **2** both exhibit intrachain antiferromagnetic couplings, which is in agreement with the rules established for most Fe^{III}–CN–Mn^{III} interactions [38], that is the orthogonality between the magnetic orbital of Fe^{III} and Mn^{III} can be lost as the bending of the Mn–N–C(cyanide) increases, leading to magnetic coupling type from ferro- to antiferromagnetic. However, the magnetic behavior for **1** and **2** at low temperature deviates significantly from that expected for typical ferrimagnetic AB chains where the divergence of $\chi_M T$ at low temperature could always be observed [58]. Such inconsistency obviously reveals that the 1-D magnetic properties of **1** and **2** at low temperature become insignificant because of the interchain interactions. In this case, the 1-D magnetic properties can be still detected of **1** (frequency dependent χ_M'' signals) but are completely invisible for **2**, indicating the intermolecular antiferromagnetic interactions in **2** are stronger than that in **1**. The magnetic properties of these two complexes are also well understood from a structural point of view. Indeed the pairs of chains are somewhat more closely packed in the crystal structure of **2** than in **1**, as illustrated in the structure analysis section.

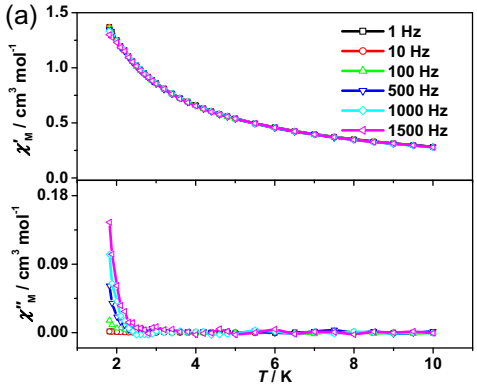

Fig. 3. The real (χ'_M) and imaginary (χ''_M) parts of AC magnetic susceptibility for **1** under 0 DC and 3 Oe AC magnetic field.

4. Conclusions

In this work, two new heterobimetallic cyano-bridged complexes **1** and **2** were constructed from *mer*-[Fe^{III}(qcq)(CN)$_3$]$^-$ and Mn^{III}(Schiff-base) building blocks. X-ray structural analysis reveals their very comparable structures featuring 1-D zigzag chain arrangement, which further extends into 3-D supramolecular networks via interchain weak interactions such as $\pi\cdots\pi$ stacking and hydrogen bond contacts. Interestingly, different Mn^{III}(Schiff-base) cations used for **1** and **2** have led to comparable zigzag chain structure but different magnetic behavior at the low temperature. Further study of such interesting systems by systematically tuning the topology of the chain is undergoing in our laboratory.

Acknowledgments

The authors are grateful for financial support from the National Natural Science Foundation of China (Nos. 51072071 and 1601310042), Doctoral Innovation Program Foundation of China (No. 1721310119) and the Startup Foundation for Advanced Talents of Jiangsu University (No. 11JDG106).

Appendix A. Supplementary material

CCDC 969347 and 969348 contain the supplementary crystallographic data for complexes **1** and **2**. These data can be obtained free of charge from The Cambridge Crystallographic Data Centre via www.ccdc.cam.ac.uk/data_request/cif. Supplementary data associated with this article can be found, in the online version, at http://dx.doi.org/10.1016/j.ica.2014.01.046.

References

[1] R. Sessoli, D. Gatteschi, A. Caneschi, M.A. Novak, Nature 365 (1993) 141.
[2] S. Hill, R.S. Edwards, N. Aliaga-Alcalde, G. Christou, Science 302 (2003) 1015.
[3] N. Roch, S. Florens, V. Bouchiat, W. Wernsdorfer, F. Balestro, Nature 453 (2008) 633.
[4] H.L. Sun, Z.M. Wang, S. Gao, Coord. Chem. Rev. 254 (2010) 1081.
[5] A. Caneschi, D. Gatteschi, R. Sessoli, A.L. Barra, L.C. Brunel, M. Guillot, J. Am. Chem. Soc. 113 (1991) 5873.
[6] A.M. Ako, I.J. Hewitt, V. Mereacre, R. Clerac, W. Wernsdorfer, C.E. Anson, A.K. Powell, Angew. Chem. Int. Ed. 45 (2006) 4926.
[7] P.H. Lin, T.J. Burchell, L. Ungur, L.F. Chibotaru, W. Wernsdorfer, M. Murugesu, Angew. Chem. Int. Ed. 48 (2009) 9489.
[8] H.L. Tsai, C.I. Yang, W. Wernsdorfer, S.H. Huang, S.Y. Jhan, M.H. Liu, G.H. Lee, Inorg. Chem. 51 (2012) 13171.
[9] A. Caneschi, D. Gatteschi, N. Lalioti, C. Sangregorio, R. Sessoli, G. Venturi, A. Vindigni, A. Rettori, M.G. Pini, M.A. Novak, Angew. Chem. Int. Ed. 40 (2001) 1760.
[10] N.E. Chakov, W. Wernsdorfer, K.A. Abboud, G. Christou, Inorg. Chem. 43 (2004) 5919.

[11] R. Lescouëzec, L.M. Toma, J. Vaissermann, M. Verdaguer, F.S. Delgado, C. Ruiz-Pérez, F. Lloret, M. Julve, Coord. Chem. Rev. 249 (2005) 2691.
[12] J. Kim, S.J. Han, J.M. Lim, K.Y. Choi, H. Nojiri, B.J. Suh, Inorg. Chim. Acta 360 (2007) 2647.
[13] L.C. Kang, X. Chen, C.F. Wang, X.H. Zhou, J.L. Zuo, X.Z. You, Inorg. Chim. Acta 362 (2009) 5195.
[14] S. Wang, J.L. Zuo, H.C. Zhou, Y. Song, X.Z. You, Inorg. Chim. Acta 358 (2005) 2101.
[15] R. Clerac, H. Miyasaka, M. Yamashita, C. Coulon, J. Am. Chem. Soc. 124 (2002) 12837.
[16] H. Miyasaka, A. Saitoh, S. Abec, Coord. Chem. Rev. 251 (2007) 2622.
[17] T. Glaser, M. Heidemeier, T. Weyhermüller, R.D. Hoffmann, H. Rupp, P. Müller, Angew. Chem. Int. Ed. 45 (2006) 6033.
[18] N. Matsumoto, Y. Sunatsuki, H. Miyasaka, Y. Hashimoto, D. Luneau, J.P. Tuchagues, Angew. Chem. Int. Ed. 38 (1999) 171.
[19] H. Miyasaka, N. Matsumoto, H. Ōkawa, N. Re, E. Gallo, C. Floriani, J. Am. Chem. Soc. 118 (1996) 981.
[20] D. Visinescu, L. Marilena, Dalton Trans. (2009) 37.
[21] H. Miyasaka, T. Madanbashi, A. Saitoh, N. Motokawa, R. Ishikawa, M. Yamashita, S. Bahr, W. Wernsdorfer, R. Clerac, Chem. Eur. J. 18 (2012) 3942.
[22] H.B. Zhou, Z.C. Zhang, Y. Chen, Y. Song, X.Z. You, Polyhedron 30 (2011) 3158.
[23] J. Dreiser, K.S. Pedersen, A. Schnegg, K. Holldack, J. Nehrkorn, M. Sigrist, P. Tregenna-Piggott, H. Mutka, H. Weihe, V.S. Mironov, J. Bendix, O. Waldmann, Chem. Eur. J. 19 (2013) 3693.
[24] J.W. Lee, K.S. Lim, D.W. Ryu, E.K. Koh, S.W. Yoon, B.J. Suh, C.S. Hong, Inorg. Chem. 52 (2013) 8677.
[25] H.Z. Kou, Z.H. Ni, C.M. Liu, D.Q. Zhang, A.L. Cui, New J. Chem. 33 (2009) 2296.
[26] Z.H. Ni, H.Z. Kou, L.F. Zhang, C. Ge, A.L. Cui, R.J. Wang, Y. Li, O. Sato, Angew. Chem. Int. Ed. 44 (2005) 7742.
[27] D. Zhang, H. Wang, L. Tian, H.Z. Kou, J. Jiang, Z.H. Ni, Cryst. Growth Des. 9 (2009) 3989.
[28] H. Miyasaka, H.I.N. Matsumoto, N. Re, R. Crescenzi, C. Floriani, Inorg. Chem. 37 (1998) 255.
[29] T. Senapati, C. Pichon, R. Ababei, C. Mathoniere, R. Clerac, Inorg. Chem. 51 (2012) 3796.
[30] J.I. Kim, H.S. Yoo, E.K. Koh, C.S. Hong, Inorg. Chem. 46 (2007) 10461.
[31] J.I. Kim, J.H. Yoon, H.Y. Kwak, E.K. Koh, C.S. Hong, Eur. J. Inorg. Chem. (2008) 2756.
[32] J.I. Kim, H.Y. Kwak, J.H. Yoon, D.W. Ryu, I.Y. Yoo, N. Yang, E.K. Koh, J.G. Park, H. Lee, C.S. Hong, Inorg. Chem. 48 (2009) 2956.
[33] I.Y. Yoo, D.W. Ryu, J.H. Yoon, A.R. Sohn, K.S. Lim, B.K. Cho, E.K. Koh, C.S. Hong, Dalton Trans. 41 (2012) 1776.
[34] H.R. Wen, Y.Z. Tang, C.M. Liu, J.L. Chen, C.L. Yu, Inorg. Chem. 48 (2009) 10177.
[35] S. Wang, M. Ferbinteanu, M. Yamashita, Inorg. Chem. 46 (2007) 610.
[36] H.Y. Kwak, D.W. Ryu, J.W. Lee, J.H. Yoon, H.C. Kim, E.K. Koh, J. Krinsky, C.S. Hong, Inorg. Chem. 49 (2010) 4632.
[37] J.I. Kim, H.S. Yoo, E.K. Koh, H.C. Kim, C.S. Hong, Inorg. Chem. 46 (2007) 8481.
[38] D. Visinescu, L.M. Toma, J. Cano, O. Fabelo, C. Ruiz-Perez, A. Labrador, F. Lloret, M. Julve, Dalton Trans. 39 (2010) 5028.
[39] D.P. Zhang, L.F. Zhang, Z.D. Zhao, X. Chen, Z.H. Ni, Inorg. Chim. Acta 377 (2011) 165.
[40] H.B. Zhou, J. Wang, H.S. Wang, Y.L. Xu, X.J. Song, Y. Song, X.Z. You, Inorg. Chem. 50 (2011) 6868.
[41] K.J. Cho, D.W. Ryu, H.Y. Kwak, J.W. Lee, W.R. Lee, K.S. Lim, E.K. Koh, Y.W. Kwon, C.S. Hong, Chem. Commun. 48 (2012) 7404.
[42] H. Miyasaka, N. Matsumoto, N. Re, E. Gallo, C. Floriani, Inorg. Chem. 36 (1997) 670.
[43] H. Miyasaka, N. Matsumoto, H. Okawa, N. Re, E. Gallo, C. Floriani, Angew. Chem. Int. Ed. 34 (1995) 1446.
[44] M. Ferbinteanu, H. Miyasaka, W. Wernsdorfer, K. Nakata, K. Sugiura, M. Yamashita, C. Coulon, R. Clerac, J. Am. Chem. Soc. 127 (2005) 3090.
[45] C. Yang, Q.L. Wang, Y. Ma, G.T. Tang, D.Z. Liao, S.P. Yan, G.M. Yang, P. Cheng, Inorg. Chem. 49 (2010) 2047.
[46] W.W. Ni, Z.H. Ni, A.L. Cui, X. Liang, H.Z. Kou, Inorg. Chem. 46 (2007) 22.
[47] S. Nastase, C. Maxim, M. Andruh, J. Cano, C. Ruiz-Perez, J. Faus, F. Lloret, M. Julve, Dalton Trans. 40 (2011) 4898.
[48] H. Miyasaka, H. Ieda, N. Matsumoto, K. Sugiura, M. Yamashita, Inorg. Chem. 42 (2003) 3509.
[49] K.S. Pedersen, M. Schau-Magnussen, J. Bendix, H. Weihe, A.V. Palii, S.I. Klokishner, S. Ostrovsky, O.S. Reu, H. Mutka, P.L. Tregenna-Piggott, Chem. Eur. J. 16 (2010) 13458.
[50] D. Zhang, H. Wang, Y. Chen, Z.H. Ni, L. Tian, J. Jiang, Inorg. Chem. 48 (2009) 11215.
[51] H.R. Wen, C.F. Wang, Y.Z. Li, J.L. Zuo, Y. Song, X.Z. You, Inorg. Chem. 45 (2006) 7032.
[52] Z.H. Ni, L.F. Zhang, V. Tangoulis, W. Wernsdorfer, A.L. Cui, O. Sato, H.Z. Kou, Inorg. Chem. 46 (2007) 6029.
[53] J. Zhang, A. Lachgar, J. Am. Chem. Soc. 129 (2007) 250.
[54] H.Y. Kwak, D.W. Ryu, H.C. Kim, E.K. Koh, B.K. Cho, C.S. Hong, Dalton Trans. (2009) 1954.
[55] H.J. Choi, J.J. Sokol, J.R. Long, Inorg. Chem. 43 (2004) 1606.
[56] T. Glaser, M. Heidemeier, E. Krickemeyer, H. Bogge, A. Stammler, R. Frohlich, E. Bill, J. Schnack, Inorg. Chem. 48 (2009) 607.
[57] P. Przychodzeń, K. Lewinski, M. Balanda, R. Pełka, M. Rams, T. Wasiutynshi, C. Guyard-Duhayon, B. Sieklucka, Inorg. Chem. 43 (2004) 2967.
[58] O. Kahn, Molecular Magnetism, VCH, New York, 1993.
[59] G.M. Sheldrick, SHELXL-97 Program for the Refinement of Crystal Structure, University of Göttingen, Göttingen, Germany, 1997.
[60] J. Seiden, J. Phys. Lett. 44 (1983) L947.
[61] J.S. Miller, M. Drillon, Magnetism: Molecules to Materials II: Molecule-Based Materials, Wiley-VCH, Weinheim, 2001.